

A Smart Sterilization Robot System With Chlorine Dioxide for Spray Disinfection

Yu-Lin Zhao^{ID}, Han-Pang Huang^{ID}, *Member, IEEE*, Tse-Lun Chen, Pen-Chi Chiang, Yi-Hung Chen, Jiann-Horng Yeh, Chien-Hsien Huang, Ji-Fan Lin, and Wei-Ting Weng

Abstract—The highly infectious and serious nature of coronavirus disease 2019 (COVID-19) has highlighted the need for hospital space disinfection technology and the prevention of human exposure to pathogenic environments. This research developed novel chlorine dioxide (ClO₂) sterilization technology to reduce bacteria and viruses in the air and on surfaces. A smart sterilization robot system was also developed to spray disinfectants in operating theaters or patients' rooms, designed according to the results of controlled experiments and the requirements for hospital disinfection. The system was built incorporated a semi-automatic remote-controlled module and an automatic intelligent disinfection function; that is, it could operate independently according to specific epidemic prevention strategies, which were implemented using a combination of Internet of Things (IoT) applications and a gesture recognition function. The elimination of *Escherichia coli* (*E. coli*) bacteria on sample plates was 99.8 % effective. This paper reviews the evolution of various disinfection technologies and describes a disinfection robot system in detail.

Index Terms—Mobile robots, medical robotics, intelligent systems, robot sensing systems.



I. INTRODUCTION

WITH the rapid development of technology and globalization, human travel and international trade are becoming more frequent. Although infectious diseases in cities may seem remote, they can be transmitted rapidly to other cities around the world through a transportation medium. According to a report by the World Health Organization (WHO) on May 25, 2021, coronavirus disease 2019 (COVID-19) had spread to 220 countries, causing 166,860,081 person-times of illness, including 3,459,996 deaths [1]. Various epidemic situations have also increased the burden and

pressure on hospitals, and effective disinfection for general wards, diagnosis rooms, halls, and examination rooms is urgently needed to prevent and control the outbreak of infectious diseases.

The disinfection methods used for various functional rooms in hospitals include manual spraying of disinfectants, ultraviolet (UV) light irradiation, and automatic disinfection robots [2]–[4]. The risk of manual disinfection is that humans may be exposed to potentially contaminated surfaces, causing anxiety, tension, and loss of productivity for medical staff, especially in hospital contagion units. Furthermore, public panic about COVID-19 has led to the popularization of disinfection robots [5]–[7]. Robot disinfection usually can be divided into two categories: UV light irradiation [8]–[10] and chemical disinfection [11], [12]. Most glass and plastics can reduce the intensity of UV radiation; thus, volatile chemical disinfectants perform better in sealed environments [4], [13], [14].

A smart sterilization robot system should be able to carry out various functions, not limited to remote movement and disinfection. Besides achieving effective disinfection, such a system should use sensor data to navigate the surrounding environment and ensure safety according to established disinfection strategies. Traditional disinfection based on human labor is restricted to the available time and attention of operators. Compared to manual disinfection, robot disinfection can be performed around the clock, even at peak times; prevent pathogenic environments or disinfectants from harming humans; and adapt to a variety of working conditions.

Manuscript received June 15, 2021; revised July 26, 2021; accepted July 26, 2021. Date of publication July 30, 2021; date of current version October 1, 2021. This work was supported in part by the Ministry of Science and Technology (MOST) of Taiwan under Grant MOST 109-2221-E-002-074-MY2. The associate editor coordinating the review of this article and approving it for publication was Dr. Eduardo Garcia-Breijo. (Corresponding author: Han-Pang Huang.)

Yu-Lin Zhao, Han-Pang Huang, and Wei-Ting Weng are with the Department of Mechanical Engineering, National Taiwan University, Taipei 106, Taiwan (e-mail: f07522844@ntu.edu.tw; hanpang@ntu.edu.tw).

Tse-Lun Chen and Pen-Chi Chiang are with the Graduate Institute of Environmental Engineering, National Taiwan University, Taipei 106, Taiwan (e-mail: pcchiang@ntu.edu.tw).

Yi-Hung Chen is with the Department of Chemical Engineering and Biotechnology, National Taipei University of Science and Technology, Taipei 106, Taiwan (e-mail: yhchen1@ntut.edu.tw).

Jiann-Horng Yeh, Chien-Hsien Huang, and Ji-Fan Lin are with Shin Kong Wu Ho-Su Memorial Hospital, Taipei 106, Taiwan (e-mail: jifanlin@hotmail.com).

Digital Object Identifier 10.1109/JSEN.2021.3101593

In order to save manpower, reduce the possibility of human exposure to the virus environment, and maximize the disinfection agent utilization efficiency and spraying effectiveness, the robot was designed to be mounted with a disinfectant spraying device and embedded a variety of sensors to sense the environment and ensure the safety of human beings and the robot itself. Finally, the semi-automatic remote-control or automatic intelligent disinfection function can be realized through the cooperation of various sections.

The research objective was to integrate practical technologies into a smart sterilization robot system to achieve the efficient disinfection that is crucial during pandemics. First, the advantages and disadvantages of disinfection methods and the characteristics of various disinfection robots were evaluated to provide the foundation for the design parameters and functionalities of our system. After the system's hardware and software had been identified, the active and passive behaviors of a robot system were defined to underpin the automatic control mechanism. An embedded computer would determine the speed of the robot system and the state of the valve on the robot according to sensor data, recognize a user's gestures, and execute commands using a camera. The robot system was ultimately tested in the field for disinfection verification and evaluation to prove that it could inhibit the growth of *E. coli* bacteria in a hospital environment.

II. FUNDAMENTALS OF THE DISINFECTION ROBOT SYSTEM

A. Disinfection Methods

Disinfection is a process that destroys or otherwise inactivates pathogenic organisms. This outcome may be achieved using different physicochemical treatments, including direct application of thermal energy, UV light irradiation, and/or chemical reagents. UV light and chemical spraying are the most common methods for disinfecting spaces. UV light can be divided into three types with different wavelengths: ultraviolet A (UVA), ultraviolet B (UVB), and ultraviolet C (UVC). UVC (with a wavelength of about 200–280 nm), which is sometimes called deep UV (DUV), is the most effective wavelength for epidemic prevention and disinfection. It destroys the deoxyribonucleic acid (DNA) and ribonucleic acid (RNA) of microorganisms through electric radiation, and then kills biological cells to achieve disinfection and sterilization. UVC is effective against all known coronaviruses [15].

UVC is produced by various types of equipment, including UV lamps, mercury vapor lamps, and UV light-emitting diodes (UV-LEDs). In the past, mercury vapor lamps were often used as UV generators, which caused serious environmental pollution due to their high energy consumption. According to the Minamata Convention on Mercury, vapor lamps are gradually being replaced by UV-LEDs, which have more concentrated energy and lower energy consumption [16], [17]. UVC is used to combat the crisis of increasing multidrug resistant organisms (MDROs) in patients' rooms, bathrooms, operating theaters (OTs), and equipment rooms, and on mobile devices [18]. Some researchers [19], [20] evaluated the efficiency of UVC for disinfection of electronic products, and

TABLE I
COMPARISON OF SPACE DISINFECTION METHODS

Disinfectant	Principle	Advantages	Disadvantages
UV light	Destroys microbial nucleic acid.	Low cost, no disinfectant consumption.	Insufficient penetration depth, may cause conjunctivitis.
NaClO	Sterilizes by chlorine substitution and oxidation reaction.	Low cost.	Corrosion of metals.
HOCl	Sterilizes by chlorine substitution and oxidation reaction.	Low toxicity, high efficiency.	High pollution, corrosion of metals.
ClO ₂	Inactivates enzymes by oxidation reaction.	Low cost, high efficiency, less residue.	Inconvenient storage.
H ₂ O ₂	Inactivates enzymes by oxidation reaction.	Low toxicity, less residue.	Inconvenient storage.
Alcohol	Dehydrates the protein in microorganisms.	Low cost, less residue.	Ineffective against enterovirus, flammable.
O ₃	Acts on cell membranes to change permeability.	High efficiency, deodorizing.	High toxicity, high costs.

UVC light effectively eliminated all the pathogenic bacteria on mobile phones.

According to [4], [13], UVC disinfection should not be used alone but could be combined with chemical disinfection. As another common approach, a chemical disinfection system is linked to many devices, including storage tanks, pumps, power supplies, different types of nozzles, and aerosol sprays. Due to the nature of aerosols, any pathogens without physical shielding would be killed. The design of spraying devices and the choice of chemical agents can also undermine the effectiveness of disinfection. According to studies [4], [14], [21]–[23], some chemical agents, such as sodium hypochlorite (NaClO), hypochlorous acid (HOCl), chlorine dioxide (ClO₂), hydrogen peroxide (H₂O₂), alcohol, and ozone (O₃), can be effective sterilizers. A comparison of various space disinfection methods is shown in TABLE I. Most disinfectants are volatile, leave little residue, and are relatively cheap. Compared to UV disinfection, ClO₂ solution particles have stronger disinfection effects. Diffusing and permeable ClO₂ aerosols are good fumigants for disinfecting confined spaces. Fogged ClO₂ disinfectant can effectively eliminate human norovirus (HoV) and feline calicivirus (FCV) on hard-to-reach surfaces [24]. Some studies [23], [25]–[29] indicated that both the aqueous and gaseous forms of ClO₂ demonstrate good sterilization efficiency. Additionally, ClO₂ has the characteristics of low cost, extremely low residue, good sterilization effects, and relative safety. Accordingly, ClO₂ solution is distributed in aerosol and fog states for disinfection.

B. Robot Technologies for Disinfection Systems

In response to the spread of COVID-19, various robots were developed for patient diagnosis and health care, food

and drug delivery, social interaction, and disinfection, which also promoted corresponding robot technologies. Robot technologies consist of communication devices, control modules, path planning tools, simultaneous localization and mapping (SLAM), and behavior monitoring. Robot platforms equipped with epidemic prevention functions usually travel on wheels or bipedal devices. Most of them are designed to complete sterilization work through remote control or a fixed route, which protects operators from harmful disinfectants while satisfying basic disinfection requirements. Some robots with cameras can be controlled to explore enclosed spaces by wireless communication protocols based on the interconnection between internal modules and external modules.

Robots generally employ various sensors, including cameras, light detection and ranging (LIDAR), inertial measurement units (IMUs), temperature sensors, proximity sensors, and humidity sensors, to observe the surrounding environment and calculate the disinfection path. Path planning may differ across types of robots; nevertheless, it is largely similar for robots intended for disinfection purposes with similar pesticide spraying strategies. One of the most common uses of robots is to pick up and place objects, which requires a start point and an end point. Path-following algorithms, such as the A*, AO*, rapidly-exploring random trees (RRTs), and DAO* algorithms, search for the best path and then execute commands accordingly [30]. Since disinfection robots need to traverse whole spaces and spray disinfectants uniformly, the first design task is to construct 2D or 3D metric maps via SLAM, which is used by robots to acquire maps of the surrounding environment and position themselves accordingly. Laser scans or images are combined to form a map based on geometric relationships, which is then decomposed into many blocks with different weightings, enabling the robot to identify obstacles and edges and avoid collisions. Finally, graph traversal is used to plan the robot's motion; for example, simultaneous localization and mapping with moving object tracking and scene prediction (SLAMMOT-SP) is an algorithm that integrates multiple robotics technologies, allowing each robot to actively predict possible changes of views and identify moving objects [31], [32].

Image recognition and robot behavior are also important functions of disinfection robots. Image recognition is a visual aid system, which should be treated as an auxiliary function requiring operator intervention. Image recognition makes the behaviors of the robots more intelligent and may permit them to work independently.

C. Disinfection Strategies

This section describes different disinfection strategies used to verify the effect of epidemic prevention, with the efficiency of the disinfection method calculated by comparing the number of bioindicators present before and after disinfection. There are many complex factors that affect the death of bioindicators, including measurement methods, disinfection equipment, disinfection times, bioindicator properties, room characteristics, etcetera. The bioindicators used for effectiveness testing, including *E. coli*, methicillin-resistant *Staphylococcus aureus* (MRSA), and multidrug resistant *Acinetobacter baumannii*,

are more resistant to disinfection but less harmful than COVID-19.

Due to the time required for biological cultivation and inspection, robots cannot carry out disinfection verification work. Verification can be used to evaluate and improve the efficiency of robots, based on counts of bioindicator populations in professional laboratories. Jinadatha *et al.* [33] showed that UV disinfection improved overall cleanliness and was better than manual cleaning for MRSA and bacterial heterotrophic plate counts (HPC). Fleming *et al.* [34] showed that UV robots had positive effects on disinfection for *Clostridium difficile* (*C. diff*).

The effectiveness of disinfection is closely related to disinfection strategies. Robots without disinfection strategies lack the necessary flexibility to deal with emergencies and complex environments, but too little research has investigated disinfection strategies and their related functions; thus, most robots are unable to manually traverse whole spaces and achieve complete sterilization. An appropriate path planning strategy, as presented by [35], is an important way to improve efficiency by calculating the efficient route according to various parameters. Hu *et al.* [36] developed a deep-learning method to distinguish between different areas of potential contamination and assign different weights to guide a robot disinfection system.

III. MATERIALS AND METHODS

A. Disinfection Experiments

Before configuring the robot, a controlled experiment was performed to determine the sterilization effect of a ClO₂ solution on bioindicators at different concentrations. The ClO₂ solution was prepared by dissolving commercial ClO₂ effervescent tablets (Green Disinfectant, Virashield Asia Limited, Hong Kong, China) in deionized water according to the instructions: one effervescent tablet in 1 l of water produced a 100 ppm ClO₂ solution with a pH value of 2.30.

The selected bioindicator *E. coli*, which has low toxicity and is easy to cultivate, is distinct from other bacteria. Wang *et al.* [37] showed that SARS-CoV is more susceptible to disinfectants than *E. coli*, indicating that *E. coli* was suitable as a biological indicator for coronavirus. The *E. coli* was coated onto porous beads and stored at -80 °C. The beads were then placed on agar plates and incubated at 37 °C for 24 h. The colony density was adjusted to 6.3×10^9 CFU/mL and stored at 4 °C before use. All the petri dishes in the experiment had a diameter of 9 cm and a bottom area of 55 cm². The sprayed ClO₂ solution had a concentration of 1,000 ppm. The log reduction and disinfection efficiency for *E. coli* were determined by comparing the survival of the populations with a control group.

The controlled experiments included a negative control and a positive control with dripping solutions at different concentrations, which eliminated most potential confounding variables. The experiments confirmed that the ClO₂ solution has a disinfecting effect on *E. coli*. The number of *E. coli* colonies is shown in TABLE II. The colonies in the two sample petri dishes were counted and marked as X₁, X₂(unit: PCS, same as in TABLE VI). The RPD indicated that the two

TABLE II
THE NUMBER OF *E. Coli* COLONIES (NEGATIVE CONTROL AND POSITIVE CONTROL)

Conditions			Experiments			
Control Type	Concentration	Drop Volume	X_1	X_2	Mean	RPD*
Negative Control	N/A	N/A	610	600	605	1.7%
Positive Control	10 ppm	1 mL	532	546	539	2.6%
Positive Control	100 ppm	1 mL	425	328	376.5	25.8%
Positive Control	1000 ppm	1 mL	0	0	0	0

* Relative percentage difference (RPD) is equal to the absolute value of the difference between X_1 and X_2 divided by the mean of X_1 and X_2 , which was used to analyze the similarity of the two sets of data.

TABLE III
THE PSEUDO-CODE FOR THE RRT-CONNECT ALGORITHM

```

connect( $S, q$ )
1 do {
2    $S = \text{extend}(S, q)$ 
3 } while ( $S = \text{Advanced}$ )
4 return  $S$ ;

RRTConnectPlanner( $q_{init}, q_{goal}$ )
1  $T_a.\text{init}(q_{init}); T_b.\text{init}(q_{goal})$ 
2 for  $k = 1$  to  $K$  do
3    $q_{rand} \rightarrow \text{randomConfig}()$ 
4   if not ( $\text{extend}(T_a, q_{rand}, q_{new}) = \text{Trapped}$ ) then
5     if ( $\text{connect}() = \text{Reached}$ ) then
6       return path( $T_a, T_b$ )
7   swap( $T_a, T_b$ )
8 return Failure;

```

sets of data were similar and that there were few accidental factors. Thus, the time for effective disinfection could be calculated according to the results of the positive control and the characteristics of the nozzle. The operational parameters and appearance of the robot were customized to ensure that the environment was disinfected and to control the consumption rate of the disinfectant simultaneously.

B. Route Planning

Robot motion planning involves a system configuration space with one or more complicated geometric bodies across which a robot must identify a collision-free path between a given starting point and a goal.

The disinfection robot was designed using a path planning method called Rapidly-Exploring Random Tree Connect (RRT-Connect) [38], which consisted of two rapidly-exploring random trees (RRTs) and a simple greedy heuristic. RRTs were used for the robot's route planning, the aim of which was to select a route from a start position (q_{init}) to a goal position (q_{goal}), preventing the robot from colliding with a target object or obstacles. A set of start-to-goal routes could be obtained using SLAM and image recognition or commands issued by an operator. Two bidirectionally extended RRTs calculated a feasible path based on random sampling, and the

TABLE IV
COMPARISON OF THE DISINFECTION ROBOTS

Disinfection methods	Robot Technologies	Applications	Experimental Effects	Ref.
UVC, 3×19.3 w	Manual navigation	Indoor disinfection	35cm, kill 23/23 <i>S. aureus</i>	[8]
UVC	Automatic navigation, manual navigation	Indoor disinfection	N/A	[9]
UVC, 4×75 w	Automatic navigation, manual navigation	Indoor disinfection	Over 16.9 mJ/cm ² , disinfect 24/24 markers	[10]
Chemical disinfectant	Manual navigation	Indoor disinfection	N/A	[11]
Chemical disinfectant	Automatic navigation, manual navigation	Animal husbandry	N/A	[12]

heuristic greedy method calculated the local optimal solution and reduced the operation time.

TABLE III shows the pseudo-code of the RRT-connect algorithm. Two trees, T_a and T_b , were built from q_{init} and q_{goal} , followed by random sampling K times. Two functions were governed by the RRT connect algorithm: 'Extend' and 'Connect'. 'Extend' created q_{new} from q_{rand} in T_a and extended from T_b to the q_{new} direction of T_a . If q_{new} collided with an obstacle, the Extend function would return empty. 'Connect' made a judgment about whether T_a and T_b were connected as a whole S ; if not, the random sampling continued until it failed.

The RRT-Connect algorithm is simple, requires few resources, and can quickly calculate a path, which met our needs. The path could be planned by giving multiple denser goals, enabling the risky environment to be disinfected.

C. Proposal for the Robot System

TABLE IV shows a comparison of disinfection robots. A robot can be equipped with UVC-LEDs for disinfection, but operators must avoid looking at the LEDs directly because they can cause eye injury in a few seconds. Chanprakon *et al.* [8] designed a UVC disinfection robot system based on Raspberry Pi, which connected to the robot via Wi-Fi to control its movements. However, UV robots have shortcomings: direct UVC exposure can cause damage to the eyes and skin. The LEDs mounted on robots build up heat, but fans and other light-shielding equipment cannot be used for heat dissipation. Even worse, disinfection is time-consuming, and it is difficult to disinfect "dead" corners blocked by obstacles or dust. The robot in this study had three 19.3-watt UV lamps and a height of 1.44 meters. In the experiment, all the *S. aureus* colonies were killed within 8 s of UV light exposure; however, the number of bacteria colonies on the reference plate was 23, and a single control group was not sufficient to ensure accuracy. Tiseni *et al.* [10] developed a novel trajectory planner based on a genetic algorithm that optimized the efficiency of radiation according to the environment. Krishnamoorthy and Tande [39] showed that the effectiveness of UVC germicidal irradiation

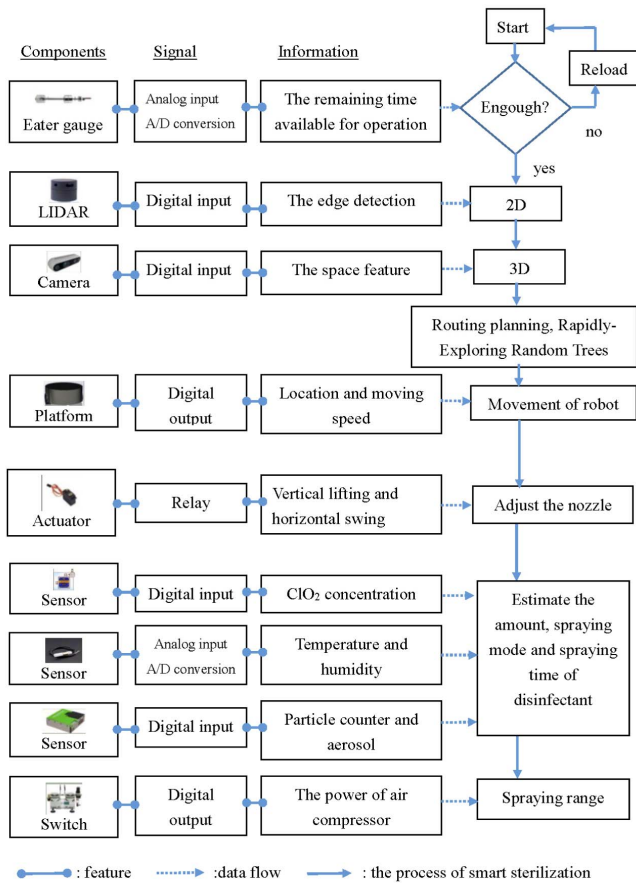


Fig. 1. The flow chart for the smart sterilization robot system.

was improved by a reflective wall coating. Buonanno *et al.* [40] estimated that UVC (at about 222 nm) could kill 99 % of coronavirus in about 16 min at the current regulatory exposure limit (~3 mJ/cm²/hour). The robot can also disinfect the environment by spraying disinfectant. Feng and Wang [12] focused on livestock breeding and established a strong flow spraying robot. Comparing various disinfection robot systems enabled us to incorporate the best aspects of architecture design, operational parameters, and various functionalities into the construction of our robot system. Moreover, we addressed deficiencies in the aforementioned studies by designing epidemic prevention strategies and conducting scientific verification of disinfection effects.

Fig. 1 shows the flow chart of the proposed smart sterilization robot system. The smart sterilization process is as follows:

1. The robot confirms whether the stock of disinfectant is sufficient to complete the next task.
2. The robot uses LIDAR and the camera to perform edge detection and spatial image feature discrimination to construct 2D or 3D metric maps via SLAM.
3. The robot plans the route and suggests the best route using the RRT algorithm.
4. Using the best route to reach the destination quickly, the robot recognizes the operator’s gesture for a different response.
5. Based on environmental sensing information, the robot evaluates the disinfection dosage, spray mode, and spray direction.



Fig. 2. The hardware for the smart sterilization robot system.

TABLE V
THE PARAMETERS OF THE SMART STERILIZATION ROBOT SYSTEM

Size	440 × 440 × 860 mm
Weight	23 kg
Battery Storage	12 × 2 + 13 Ah
Endurance	Over 1 h
Spray Capacity	5 L/h
Vertical Lifting Range	800 mm–1,000 mm
Horizontal Swing Range	-40°–140°
Disinfectant Cost Estimate	1–3 USD per liter

6. The operator remotely controls the height and elevation of the nozzle for disinfection operation.

7. The CIO₂ concentration determined by the environment sensor will be fed back to control air compressor actuation.

As shown in Fig. 2, the whole system rests on a mobile robot platform, which supports the weight of all the modules. The wheels of the platform can bear a weight of 50 kg and move freely across the flat surface. The left and right motors are driven by 12-volt batteries. Raspberry Pi controls the motors and LIDAR SLAM map generation. The complete robot design parameters are shown in TABLE V. A CIO₂ solution with a concentration of 1,000 ppm costs about 1–3 USD per liter. The robot is also equipped with two computers: a NVIDIA Jetson NX Xavier and an Intel Core i7-9700TE (4 cores @ 1.8GHz), which are respectively used for IoT sensor signal processing and image recognition. Extra computing power and interfaces are reserved for extension of the hardware and software, such as for machine learning and additional sensors.

The graphical user interface (GUI) for the smart sterilization robot system is shown in Fig. 3. The robot can be controlled

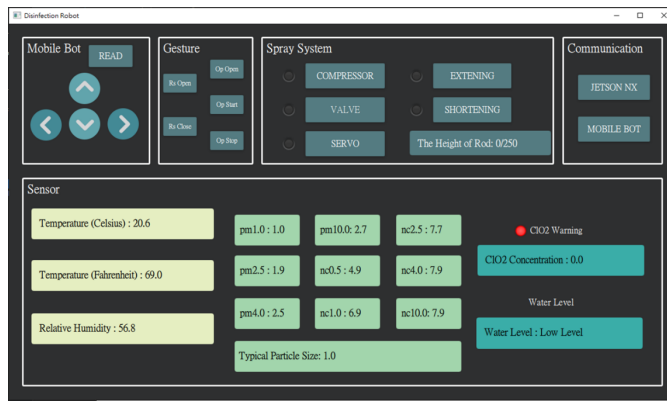


Fig. 3. The graphical user interface (GUI) for the smart sterilization robot system.

and monitored through the GUI, which can be used on an external laptop, or on a computer mounted on the robot. A socket is used for communication inside the robot and is also responsible for the transmission of sensor values and for controlling signals.

IV. DEVELOPMENT OF DISINFECTION ROBOT SYSTEM

A. IoT Sensors and Control System

The disinfection robot system is equipped with IoT sensors to assess environmental information for surrounding perception, allowing the corresponding disinfection strategies to be designed accordingly. These sensors include a temperature and humidity sensor, a particulate matter (PM) sensor, a ClO_2 concentration sensor, and a water level gauge. The values obtained by these sensors are used for the feedback control of the travel speed, location, and spray unit of the robot platform.

The disinfectant spray module comprises a pressure water tank, a small air compressor, a two-fluid nozzle, motors, and IoT sensors. The motors provide two degrees of freedom (DoFs) for control, allowing the nozzle to move vertically and swing horizontally to increase the spray range. Air compressors and electric valves are also controllable devices. During the test, the actual spray rate was about 1.4 mL per second, the aerosol particle size was about 20 to 30 μm , and the coverage radius was about 1 meter.

This robot system can use multiple disinfectants, but the evaluation showed that ClO_2 is relatively the best choice. ClO_2 disinfectant is a strong oxidant with antimicrobial activity and is expected to serve as an inexpensive option for cleaning and disinfecting hospital environments. Compared with chlorine-based disinfectants that rely on chlorination reactions for disinfection, ClO_2 disinfection products, relying on oxidation reactions, have no carcinogenic effects. Although ClO_2 is inconvenient to store and transport, this is not a concern for a robot system structurally equipped with a Hi-Gee module. The Hi-Gee module—a small high-gravity rotating packed bed for producing ClO_2 gas—can be configured as a standalone product used for disinfection.

B. SLAM and Image Recognition

Robots without SLAM and image recognition functionality cannot operate independently. SLAM involves two types of

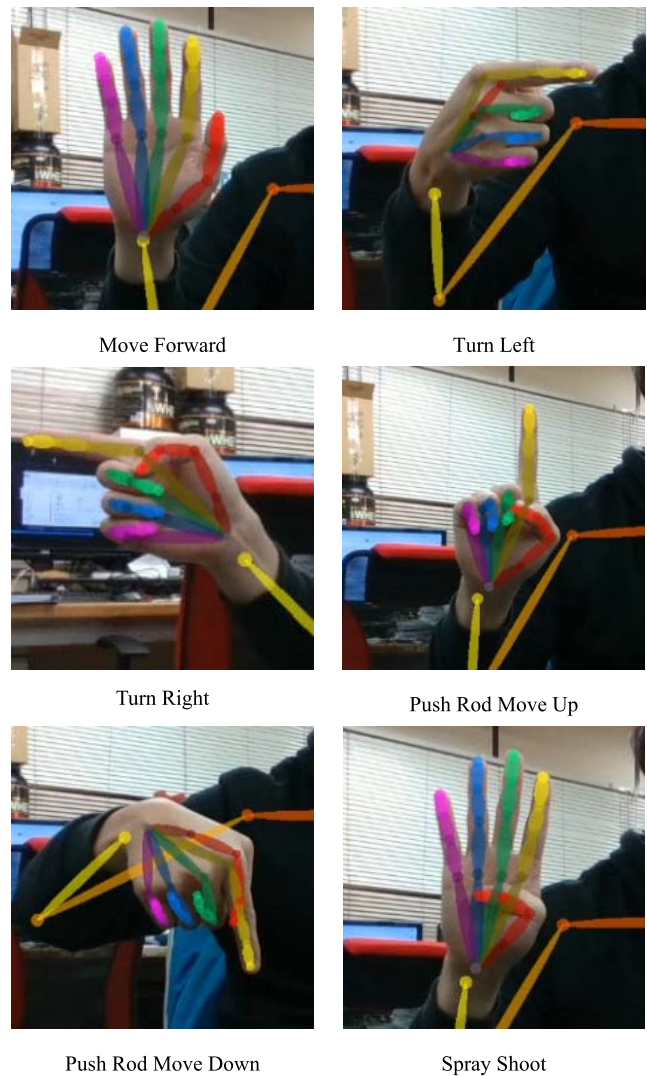


Fig. 4. Hand gestures and corresponding commands.

devices: one is 2D SLAM using Flash LIDAR F4 and the other is 3D SLAM using an Intel RealSense Depth Camera D435i. The 2D SLAM in the system is mainly based on Robot Operating System (ROS) [41] and GMapping algorithm [42], [43], which is a more reliable and mature algorithm based on LIDAR and odometer solutions. The core of the GMapping algorithm is a particle filter, which helps to calculate the distribution of variables by combining samples with parameter density functions. 3D SLAM, based on ORB-SLAM [44], [45], is combined with Point Cloud Library (PCL) [46] to display the internal structure of the room. During the experiment, the robot could avoid obstacles, including pedestrians, in real time. Due to the error and bias of the odometer and LIDAR or the robot's slipping motion, the robot coordinates estimated by 2D SLAM were not accurate. Sensor fusion was used to correct this error. The matrices of poses calculated by 2D and 3D SLAM are loosely coupled with different weights, which makes the system more accurate and robust.

Image recognition and hand gesture control were developed for the robot system (Fig. 4). The gesture recognition was based on OpenPose [47]. The images from the camera stream are processed into feature vectors, which are used to match

those of defined gestures. The best similarity between multiple consecutive frames is used to make the final judgment. As a result, the robot could be manipulated to perform many tasks, such as displacement, spraying disinfectant, and so on.

C. Disinfection Strategies

Alongside the construction of the body of the robot system, the key to its intelligence lies in the design and implementation of disinfection strategies, which use data returned by IoT sensors for feedback control, image recognition of user gestures, and execution of commands.

Disinfection strategies based on IoT sensors do not require human interaction and are described as follows. Changes in temperature and humidity in the air are the two important factors affecting disinfection effectiveness and were used to determine the optimal exposure time for disinfection. The Occupational Safety and Health Administration (OSHA) suggested the health standard of 0.1 ppm averaged over 8 h of ClO₂ exposure in 2002 [48], and excessive inhalation of ClO₂ gas may cause many problematic symptoms, such as coughing, sore throat, and severe headaches [23]; hence, the robot is equipped with a ClO₂ concentration sensor with a measurement range of 0 to 2 ppm, which can alert the user to avoid over-inhalation. The PM sensor provides data on particle mass concentration and number count. These data serve two useful purposes: 1) Before the disinfection process, the particle concentration of each room can be roughly estimated. The results of [49] showed that COVID-19 aerosols were mainly available in two size ranges: from 0.25 μm to 1.0 μm and over 2.5 μm. Therefore, an epidemic prevention strategy can be planned so that the linear velocity of the robot can be set negatively relative to the PM data. 2) During the disinfection process, the value fluctuation of the PM sensor can indicate changes in the ClO₂ concentration in a room. Finally, the readings of the water level gauge can indicate the remaining capacity of the robot.

Path planning is an important part of intelligent disinfection. All nodes are marked and traversed using a 2D map, and the planned path can be obtained by connecting the nodes. During the experiment, the robot could follow this path to carry out disinfection, ensuring that all the possible “dead” corners were covered with minimal consumption of disinfectant.

Also, since the robot should be able to interact with operators and facial touches are frequent for human beings, it is important to disinfect the operators’ hands for epidemic prevention, so we considered and incorporated this feature. The operator uses different hand gestures (shown in Fig. 4) to direct the robot and adjust the height of the nozzle for comfortable operation; thus, the nozzle sprays low-concentration atomized ClO₂ onto the operator’s hands and should also be able to spray alcohol.

V. STERILIZATION EFFECTS VERIFICATION

The disinfection experiments were conducted in the Shin Kong Memorial Wu Ho-Su Hospital in Taipei city. The preparation of the ClO₂ solution and *E. coli* petri dishes used in the verification experiment were carried out as in the control experiment.

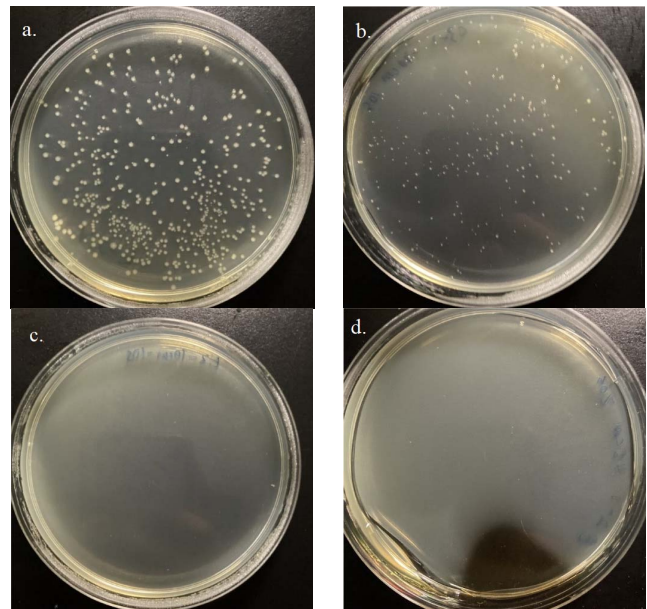


Fig. 5. Images of petri dishes under different conditions: a) negative control; b) placed vertically (vertical distance -10 cm, horizontal distance 40 cm, for 10 seconds); c) placed vertically (vertical distance -10 cm, horizontal distance 10 cm, for 10 seconds); d) placed horizontally, (vertical distance -30 cm, horizontal distance 45 cm, for 20 seconds).

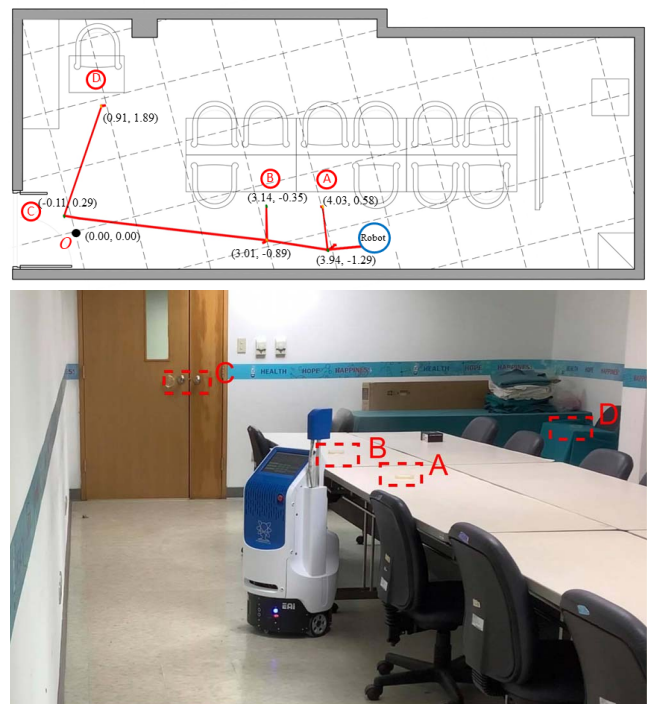


Fig. 6. The demonstration of disinfection process.

Assuming that the solution was sprayed evenly, about 0.01 mL of liquid was sprayed into the petri dish under test every second. Since pathogens can be found in many areas (especially on tables and door handles frequently touched during human activities), we estimated that the best spraying effect could be achieved by aiming the geometric central point of the spray nozzle for about 10 s. To simulate the disinfection of tables and door handles, the experimental objects were

TABLE VI
THE NUMBER OF *E. Coli* COLONIES (EXPERIMENTAL GROUPS)

Conditions				Experiments				
Petri Dish Orientation	Horizontal Distance*	Vertical Distance*	Disinfection Time	X_1	X_2	Mean	RPD**	Sterilization Rate
Negative Control	N/A	N/A	N/A	519	504	511.5	2.9 %	N/A
Horizontal	60 cm	-30 cm	5 s	221	213	217	3.7 %	57.6 %
Horizontal	60 cm	-30 cm	10 s	162	167	164.5	3.0 %	67.8 %
Horizontal	60 cm	-30 cm	20 s	1	0	0.5	200.0 %	99.9 %
Horizontal	45 cm	-30 cm	10 s	68	19	43.5	112.6 %	91.5 %
Horizontal	45 cm	-30 cm	20 s	0	0	0	0.0 %	100.0 %
Vertical	40 cm	-10 cm	10 s	3	3	3	0.0 %	99.4 %
Vertical	40 cm	-25 cm	10 s	72	67	69.5	7.2 %	86.4 %
Vertical	40 cm	-40 cm	10 s	217	230	223.5	5.8 %	56.3 %
Vertical	20 cm	-10 cm	10 s	0	0	0	0.0 %	100.0 %
Vertical	20 cm	-25 cm	10 s	46	43	44.5	6.7 %	91.3 %

*Horizontal distance and vertical distance refer to the distance between the petri dish and the nozzle.

**RPD is equal to the absolute value of the difference between X_1 and X_2 divided by the mean of X_1 and X_2 , which was used to analyze the similarity of the two sets of data.

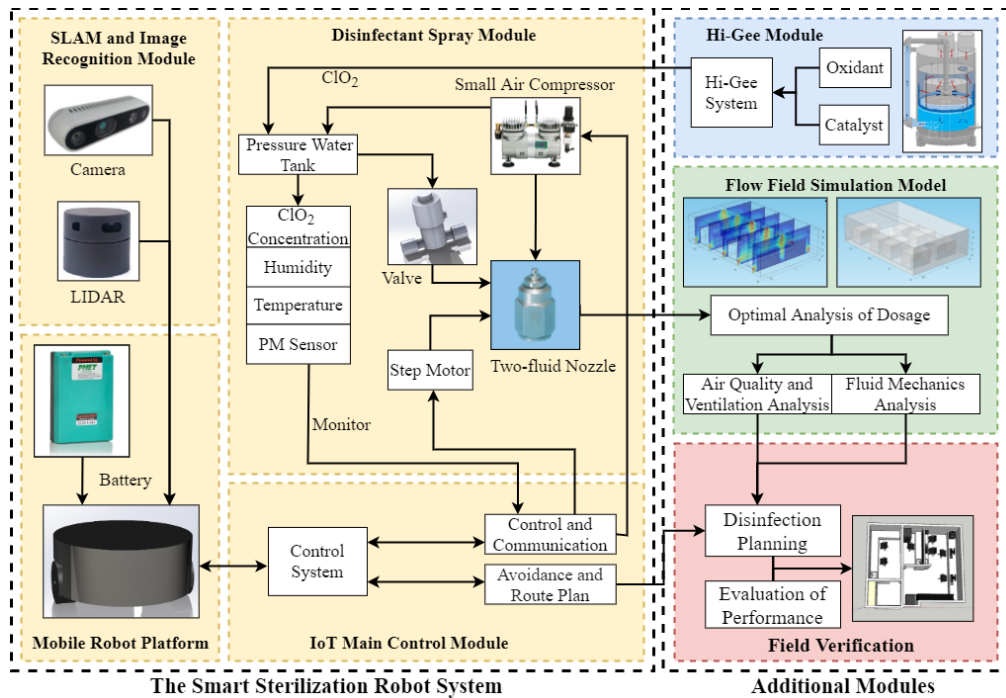


Fig. 7. The final structure of the smart sterilization robot system and additional modules.

divided into two categories: horizontal groups and vertical groups, respectively. For the horizontal groups, the nozzle was fixed at a height of 100 cm from ground level, and the petri dishes were placed on a table 30 cm lower. The control variables were disinfection time and horizontal distance. For the vertical groups, the petri dish was placed upright, and the control variables were disinfection time and the relative vertical and horizontal distances. Fig. 5 shows some examples of *E. coli* experimental groups in the petri dishes being effectively eliminated. TABLE VI shows the numbers of *E.*

coli bacteria in the colonies. The sterilization rate was equal to the mean of X_1 and X_2 minus the mean of the negative control (the number of *E. coli* theoretically killed) divided by the mean of X_1 and X_2 . The Experimental results showed that the disinfection robot can achieve effective disinfection with a sterilization efficiency above 99.8 % (510/511). Fig. 6 illustrates a demonstration of the disinfection process in the hospital. The coordinates of the goals were entered into the RRT-Connect algorithm to determine the robot's trajectory, which is marked by the red line. Point *O* is the origin of

the map when building the map, so the coordinates are (0.00, 0.00) to extend the grid line, and the unit is a meter. The robot followed the route and disinfected the petri dishes in alphabetical order. Dishes A and B were placed horizontally on the table; Dish C, simulating the disinfection of a door handle, was placed vertically; and Dish D represented the disinfection of a seat.

VI. CHALLENGES AND PROSPECTS

To respond to the outbreak of the COVID-19 pandemic and carry out prevention work, the main challenge was to rapidly develop a smart sterilization robot to satisfy the disinfection demands of hospitals. The proposed system includes hardware, software, a GUI, and disinfection strategies to achieve this. The secondary challenge was to verify the effectiveness of the robot system in a hospital. Scientific experiments facilitated the identification of the best system design and configuration to achieve ultimate disinfection efficiency.

This paper proposes a smart sterilization robot system to efficiently and stably disinfect spaces that may contain pathogenic microorganisms. The robot system incorporates multiple technologies, including IoT, aerosol disinfection, SLAM, image recognition, a control system, route planning and navigation, etc. The proposed disinfection strategy enables the robot to automatically complete disinfection throughout any target environment, thereby ensuring human safety and reducing the labor involved in manual disinfection.

Fig. 7 shows the final architecture of the smart sterilization robot system and additional modules that could be employed. The Hi-Gee module and field verification will be included in the robot system for disinfection and to analyze efficiency, respectively. Also, a simulation model of the flow field in the space should be included in the robot system as a part of the disinfection strategy. In summary, future work could include adding new sensors, such as a carbon dioxide sensor, through the reserved sensor interface to monitor human activities, and adjusting the disinfection time for different environmental conditions to enhance disinfection efficacy. Combined with the high-precision ClO₂ sensor, more disinfection experiments should be carried out to obtain accurate parameters for the robot. Furthermore, for the disinfection of various objects in a given space, such as tables, door handles, and mice, object recognition in real time could be integrated into the system to make the robot system more intelligent.

ACKNOWLEDGMENT

The authors would like to thank Chih-Hung Huang with the National Taipei University of Technology for providing disinfectant and petri dishes for us. Gratitude is also extended to the field support personnel from Shin Kong Memorial Wu Ho-Su Hospital and for the instruction of Cheng-Yun Cheng and Po-Lin Yang at the National Taiwan University Robotics Laboratory.

REFERENCES

- [1] World Health Organization. (2021). *Weekly Operational Update on COVID-19*. Accessed: May 24 2021. [Online]. Available: <https://www.who.int/publications/m/item/weekly-operational-update-on-covid-19—24-may-2021>
- [2] C. Rock, F. the CDC Prevention Epicenters Program, B. A. Small, and K. A. Thom, "Innovative methods of hospital disinfection in prevention of healthcare-associated infections," *Current Treatment Options Infectious Diseases*, vol. 10, no. 1, pp. 65–77, Mar. 2018.
- [3] J. M. Boyce, "Modern technologies for improving cleaning and disinfection of environmental surfaces in hospitals," *Antimicrobial Resistance Infection Control*, vol. 5, no. 1, pp. 1–10, Dec. 2016.
- [4] D. Armellino, K. Goldstein, L. Thomas, T. J. Walsh, and V. Petraitis, "Comparative evaluation of operating room terminal cleaning by two methods: Focused multivector ultraviolet (FMUV) versus manual-chemical disinfection," *Amer. J. Infection Control*, vol. 48, no. 2, pp. 147–152, Feb. 2020.
- [5] M. Cardona, F. Cortez, A. Palacios, and K. Cerros, "Mobile robots application against COVID-19 pandemic," in *Proc. IEEE ANDESCON*, Oct. 2020, pp. 1–5.
- [6] Z. Zeng, P. J. Chen, and A. A. Lew, "From high-touch to high-tech: COVID-19 drives robotics adoption," *Tour. Geogr.*, vol. 22, no. 3, pp. 724–734, 2020.
- [7] P. Courtney and P. G. Royall, "Using robotics in laboratories during the COVID-19 outbreak: A review," *IEEE Robot. Autom. Mag.*, vol. 28, no. 1, pp. 28–39, Mar. 2021.
- [8] P. Chanprakon, T. Sae-Oung, T. Treebupachatsakul, P. Hannanta-Anan, and W. Piyawattanametha, "An ultra-violet sterilization robot for disinfection," in *Proc. 5th Int. Conf. Eng., Appl. Sci. Technol. (ICEAST)*, Jul. 2019, pp. 1–4.
- [9] M. Guettari, I. Gharbi, and S. Hamza, "UVC disinfection robot," *Environ. Sci. Pollut. Res.*, to be published. [Online]. Available: <https://link.springer.com/article/10.1007/s11356-020-11184-2>, doi: 10.1007/s11356-020-11184-2.
- [10] L. Tiseni, D. Chiaradia, M. Gabardi, M. Solazzi, D. Leonardis, and A. Frisoli, "UV-C mobile robots with optimized path planning: Algorithm design and on-field measurements to improve surface disinfection against SARS-CoV-2," *IEEE Robot. Autom. Mag.*, vol. 28, no. 1, pp. 59–70, Mar. 2021.
- [11] M. Mohammed, I. S. Arif, S. Al-Zubaidi, S. H. K. Bahrain, A. Sairah, and Y. Eddy, "Design and development of spray disinfection system to combat coronavirus (COVID-19) using IoT based robotics technology," *Revista Argentina de Clinica Psicológica*, vol. 29, no. 5, p. 228, 2020.
- [12] Q. C. Feng and X. Wang, "Design of disinfection robot for livestock breeding," *Procedia Comput. Sci.*, vol. 166, pp. 310–314, Jan. 2020.
- [13] B. M. Andersen, H. Bånrud, E. Bøe, O. Bjordal, and F. Drangsholt, "Comparison of UV C light and chemicals for disinfection of surfaces in hospital isolation units," *Infection Control Hospital Epidemiol.*, vol. 27, no. 7, pp. 729–734, Jul. 2006.
- [14] J. Wang *et al.*, "Disinfection technology of hospital wastes and wastewater: Suggestions for disinfection strategy during coronavirus disease 2019 (COVID-19) pandemic in China," *Environ. Pollut.*, vol. 262, Jul. 2020, Art. no. 114665.
- [15] M. Heßling, K. Hönes, P. Vatter, and C. Lingenfelder, "Ultraviolet irradiation doses for coronavirus inactivation—review and analysis of coronavirus photoinactivation studies," *GMS Hyg Infect Control*, vol. 15, p. Doc08, May 2020.
- [16] X. Li, M. Cai, L. Wang, F. Niu, D. Yang, and G. Zhang, "Evaluation survey of microbial disinfection methods in UV-LED water treatment systems," *Sci. Total Environ.*, vol. 659, pp. 1415–1427, Apr. 2019.
- [17] R. Kessler, *The Minamata Convention on Mercury: A First Step toward Protecting Future Generations*. Durham, NC, USA: National Institute of Environmental Health Sciences, 2013.
- [18] A. Begić, "Application of service robots for disinfection in medical institutions," in *Advanced Technologies, Systems, and Applications II*. Cham, Switzerland: Springer, 2018, pp. 1056–1065.
- [19] L. M. Li, T. Wong, E. Rose, G. Wickham, and E. Bryce, "Evaluation of an ultraviolet C light-emitting device for disinfection of electronic devices," *Amer. J. Infection Control*, vol. 44, no. 12, pp. 1554–1557, Dec. 2016.
- [20] S. Malhotra *et al.*, "Shining a light on the pathogenicity of health care providers' mobile phones: Use of a novel ultraviolet-C wave disinfection device," *Amer. J. Infection Control*, vol. 48, no. 11, pp. 1370–1374, Nov. 2020.
- [21] B. V. Sarada, R. Vijay, R. Johnson, T. N. Rao, and G. Padmanabham, "Fight against COVID-19: ARCI's technologies for disinfection," *Trans. Indian Nat. Acad. Eng.*, vol. 5, no. 2, pp. 349–354, Jun. 2020.
- [22] M. H. Al-Sayah, "Chemical disinfectants of COVID-19: An overview," *J. Water Health*, vol. 18, no. 5, pp. 843–848, Oct. 2020.
- [23] T.-L. Chen, Y.-H. Chen, Y.-L. Zhao, and P.-C. Chiang, "Application of gaseous ClO₂ on disinfection and air pollution control: A mini review," *Aerosol Air Qual. Res.*, vol. 20, no. 11, pp. 2289–2298, 2020.

- [24] N. Montazeri, C. Manuel, E. Moorman, J. R. Khatiwada, L. L. Williams, and L.-A. Jaykus, "Virucidal activity of fogged chlorine dioxide- and hydrogen peroxide-based disinfectants against human norovirus and its surrogate, feline calicivirus, on hard-to-reach surfaces," *Frontiers Microbiol.*, vol. 8, p. 1031, Jun. 2017.
- [25] J. Huang, L. Wang, N. Ren, F. Ma, and Juli, "Disinfection effect of chlorine dioxide on bacteria in water," *Water Res.*, vol. 31, no. 3, pp. 607–613, Mar. 1997.
- [26] C.-S. Hsu, M.-C. Lu, and D.-J. Huang, "Disinfection of indoor air microorganisms in stack room of university library using gaseous chlorine dioxide," *Environ. Monitor. Assessment*, vol. 187, no. 2, p. 17, Feb. 2015.
- [27] N. Ogata *et al.*, "Inactivation of airborne bacteria and viruses using extremely low concentrations of chlorine dioxide gas," *Pharmacology*, vol. 97, nos. 5–6, pp. 301–306, Mar. 2016.
- [28] M.-C. Lu, P.-L. Chen, D.-J. Huang, C.-K. Liang, C.-S. Hsu, and W.-T. Liu, "Disinfection efficiency of hospital infectious disease wards with chlorine dioxide and hypochlorous acid," *Aerobiologia*, vol. 37, no. 1, pp. 29–38, Mar. 2021.
- [29] I. Ofori, S. Maddila, J. Lin, and S. B. Jonnalagadda, "Chlorine dioxide oxidation of *Escherichia coli* water—A study of the disinfection kinetics and mechanism," *J. Environ. Sci. Health, A*, vol. 52, no. 7, pp. 598–606, Jun. 2017.
- [30] S.-Y. Chung and H.-P. Huang, "Robot motion planning in dynamic uncertain environments," *Adv. Robot.*, vol. 25, nos. 6–7, pp. 849–870, Jan. 2011.
- [31] S. Y. Chung and H. P. Huang, "Simultaneous topological map prediction and moving object trajectory prediction in unknown environments," in *Proc. IEEE/RSS Int. Conf. Intell. Robots Syst.*, Sep. 2008, pp. 1594–1599.
- [32] S.-Y. Chung and H.-P. Huang, "SLAMMOT-SP: Simultaneous SLAM-MOT and scene prediction," *Adv. Robot.*, vol. 24, no. 7, pp. 979–1002, Jan. 2010.
- [33] C. Jinadatha, R. Quezada, T. W. Huber, J. B. Williams, J. E. Zeber, and L. A. Copeland, "Evaluation of a pulsed-xenon ultraviolet room disinfection device for impact on contamination levels of methicillin-resistant *Staphylococcus aureus*," *BMC Infectious Diseases*, vol. 14, no. 1, p. 187, Dec. 2014.
- [34] M. Fleming *et al.*, "Deployment of a touchless ultraviolet light robot for terminal room disinfection: The importance of audit and feedback," *Amer. J. Infection Control*, vol. 46, no. 2, pp. 241–243, Feb. 2018.
- [35] R. Lal, A. Sharda, and P. Prabhakar, "Optimal multi-robot path planning for pesticide spraying in agricultural fields," in *Proc. IEEE 56th Annu. Conf. Decis. Control (CDC)*, Dec. 2017, pp. 5815–5820.
- [36] D. Hu, H. Zhong, S. Li, J. Tan, and Q. He, "Segmenting areas of potential contamination for adaptive robotic disinfection in built environments," *Building Environ.*, vol. 184, Oct. 2020, Art. no. 107226.
- [37] X.-W. Wang *et al.*, "Study on the resistance of severe acute respiratory syndrome-associated coronavirus," *J. Virolog. Methods*, vol. 126, nos. 1–2, pp. 171–177, 2005.
- [38] J.-G. Kang, D.-W. Lim, Y.-S. Choi, W.-J. Jang, and J.-W. Jung, "Improved RRT-connect algorithm based on triangular inequality for robot path planning," *Sensors*, vol. 21, no. 2, p. 333, Jan. 2021.
- [39] G. Krishnamoorthy and B. M. Tande, "Improving the effectiveness of ultraviolet germicidal irradiation through reflective wall coatings: Experimental and modeling based assessments," *Indoor Built Environ.*, vol. 25, no. 2, pp. 314–328, Apr. 2016.
- [40] M. Buonanno, D. Welch, I. Shuryak, and D. J. Brenner, "Far-UVC light (222 nm) efficiently and safely inactivates airborne human coronaviruses," *Sci. Rep.*, vol. 10, no. 1, Dec. 2020, Art. no. 10285.
- [41] M. Quigley, J. Faust, T. Foote, and J. Leibs, "ROS: An open-source robot operating system," in *Proc. ICRA Workshop Open Source Softw.*, Kobe, Japan, vol. 3, 2009, p. 5.
- [42] S. Särkkä, A. Vehtari, and J. Lampinen, "Rao-Blackwellized particle filter for multiple target tracking," *Inf. Fusion*, vol. 8, no. 1, pp. 2–15, Jan. 2007.
- [43] B. L. E. A. Balasuriya *et al.*, "Outdoor robot navigation using gmapping based SLAM algorithm," in *Proc. Moratuwa Eng. Res. Conf. (MERCOn)*, Apr. 2016, pp. 403–408.
- [44] R. Mur-Artal, J. M. M. Montiel, and J. D. Tardós, "ORB-SLAM: A versatile and accurate monocular SLAM system," *IEEE Trans. Robot.*, vol. 31, no. 5, pp. 1147–1163, Oct. 2015.
- [45] R. Mur-Artal and J. D. Tardós, "ORB-SLAM2: An open-source slam system for monocular, stereo, and RGB-D cameras," *IEEE Trans. Robot.*, vol. 33, no. 5, pp. 1255–1262, Oct. 2017.
- [46] R. B. Rusu and S. Cousins, "3D is here: Point cloud library (PCL)," in *Proc. IEEE Int. Conf. Robot. Autom.*, May 2011, pp. 1–4.
- [47] Z. Cao, G. Hidalgo, T. Simon, S. E. Wei, and Y. Sheikh, "OpenPose: Realtime multi-person 2D pose estimation using part affinity fields," *IEEE Trans. Pattern Anal. Mach. Intell.*, vol. 43, no. 1, pp. 172–186, Jan. 2021.
- [48] H. Gupta, D. Bhardwaj, H. Agrawal, V. A. Tikkiwal, and A. Kumar, "An IoT based air pollution monitoring system for smart cities," in *Proc. IEEE Int. Conf. Sustain. Energy Technol. (ICSET)*, Feb. 2019, pp. 173–177.
- [49] Y. Liu *et al.*, "Aerodynamic analysis of SARS-CoV-2 in two Wuhan hospitals," *Nature*, vol. 582, no. 7813, pp. 557–560, Jun. 2020.



Yu-Lin Zhao was born in Shenyang, China, in 1996. He received the B.E. degree from the Department of Automation Engineering, National Formosa University, Taiwan, in 2018. He is currently pursuing the Ph.D. degree with the Department of Mechanical Engineering, National Taiwan University (NTU), Taiwan. He is working on robotics, the Internet of Things technology, and image recognition. He has published two papers as the first author and holds a patent.



Han-Pang Huang (Member, IEEE) received the Ph.D. degree in electrical engineering from the University of Michigan, Ann Arbor, MI, USA, in 1986. Since 1986, he has been with the National Taiwan University, Taipei, Taiwan, where he is currently a Distinguished Professor and the Zhong Zhuo-Zhang Chair Professor with the Department of Mechanical Engineering and the Graduate Institute of Industrial Engineering. He has authored more than 390 papers on these topics that have been published in refereed technical journals and conference proceedings.

His current research interests include machine intelligence, humanoid robots, intelligent robotic systems, prosthetic hands, manufacturing automation, nanomanipulation, and nonlinear systems. He is a Fellow of the Chinese Institute of Automation Engineers, the Chinese Society of Mechanical Engineers, and the Robotics Society of Taiwan.



Tse-Lun Chen was born in Taipei, Taiwan, in 1988. He received the M.S. degrees in environmental engineering from the National Taiwan University, in 2012 and 2021. From 2014 to 2017, he was an Environmental Engineer with Environmental Science and Technology Corporation. From 2019 to 2020, he has been a Visiting Researcher with the Argonne National Laboratory, USA. He is a Young Potential Researcher in the field of environmental and energy engineering. Since 2018, he has been published

11 articles in the peer-reviewed *SCI Journals*. His research interests include intensified air pollution control with high-gravity technology, air quality monitoring, electrokinetic separation and purification process, CO₂ mineralization and utilization, and greenhouse gas reduction strategies.

His awards and honors include German Academic Exchange Service (DAAD) summer scholarship in 2019, three Best Paper Awards at the Chinese Institute of Environmental Engineering Annual meeting, and one Certificate of OCEESA Best Paper Award recognized by Overseas Chinese Environmental Engineers and Scientists Association (OCEESA).



Pen-Chi Chiang received the Ph.D. degree in civil engineering from Purdue University in 1982. He is a Distinguished Professor of the Graduate Institute of Environmental Engineering, National Taiwan University (NTU), where he is the Director of the Carbon Cycle Research Center. He has worked on establishment of policies and strategies for deploying sustainable development and green technology, Taiwan. He has been published more than 220 SCI papers in the above areas since 1990. His current interests include

green infrastructure, green building, healthy watershed management, cleaner production, CO₂ capture and utilization, and energy-efficient water purification technologies.



Yi-Hung Chen was born in Taipei, Taiwan, in 1976. He received the bachelor's degree in chemical engineering and the Ph.D. degree in environmental engineering from the National Taiwan University, Taipei, in 1998 and 2003, respectively. During his Ph.D. course, his research activity concerned the pollution control and biodiesel. In 2008, he joined as the Staff of the Department of Chemical Engineering and Biotechnology, National Taipei University of Technology, Taipei. He was involved in the scientific interests of rotating packed bed, chlorine dioxide, and carbon capture and storage.

and storage.



Jiann-Horng Yeh became a Board-Certified Neurologist in 1993 after completion of residency training program with the National Taiwan University Hospital, Taipei, Taiwan. He worked as the Secretary-General of the Taiwan Neurological Society from 2001 to 2003. He is currently the Deputy Superintendent of Education and Research with Shin Kong Wu Ho-Su Memorial Hospital and a Professor and also the Associate Dean with the College of Medicine, Fu Jen Catholic University.

He has focused his research interest on myasthenia gravis after a brief fellowship training with the Institute of Molecular Medicine, University of Oxford, U.K., in 2003. He and his mentor, Prof. Hou-Chang Chiu, have set up the biggest center for myasthenia gravis care based on the vertical integration of the diagnosis, treatment, emotional management, and social rehabilitation.



Chien-Hsien Huang received the M.D. degree from the School of Medicine, Kaohsiung Medical University, Kaohsiung, Taiwan. He is a doctor of infection control and infectious diseases in Shin Kong Wu Ho-Su Memorial hospital now.

From 1998 to 2000, he was a Research Fellow of Infectious Diseases with the Department of Internal Medicine, Taipei Veterans General Hospital. He has been an attending physician since 2001 and has been the Chief of Section of Infectious Diseases with the Department of Internal Medicine, Shin Kong Wu Ho-Su Memorial Hospital since 2016. Since 2021, he has been the Secretary-General of the Infectious Diseases Society of Taiwan. His research interests include microbiology, infection control, clinical infectious diseases and acquired immune deficiency syndrome.



Ji-Fan Lin received the M.S. degree in biotechnology from the National Ocean University, New Taipei, in 1999, and the Ph.D. degree in life science from the National Defense Medical Center, in 2008.

He is currently the Deputy Director of the Research Department, Shin-Kong WHS Memorial Hospital (SKH), Taipei, Taiwan. Since 2017, he has been an Assistant Professor with the Ph.D. program in pharmaceutical biotechnology with Fu Jen Catholic University, New Taipei, Taiwan. From 2009 to 2019, he was the Principle Investigator with the Laboratory of Urological and Reproductive Medicine, SKH. In 2015, he was assigned to establish the Shin-Kong Innovation and Incubation Center, SKH (SKHIIC), where he was appointed as the Deputy Director. He was also in charge of the establishment of Shin-Kong Precision Medicine Center (SKHPMC) in 2019, where he was appointed as the Deputy Director. He is the author of more than 80 articles and holds one patent. His research interest includes dysregulated micro-RNAs and the signal transduction of autophagy related to urological cancers.



Wei-Ting Weng was born in New Taipei, Taiwan, in 1996. He received the B.E. degree from the Department of Mechanical Engineering, National Chung Hsing University, Taiwan, in 2019. He is currently pursuing the M.S. degree with the Department of Mechanical Engineering, National Taiwan University (NTU), Taiwan. He is working on robotics laboratory. His research direction is vision applied to wheeled robots.